Deposition of nickel films on polycrystalline copper alloy with various current densities from watts solution

Cite as: AIP Conference Proceedings **2331**, 030017 (2021); https://doi.org/10.1063/5.0041640
Published Online: 02 April 2021

Ferry Budhi Susetyo, Bambang Soegijono, Yusmaniar, et al.

Deposition of Nickel Films on Polycrystalline Copper Alloy with Various Current Densities from Watts Solution

Ferry Budhi Susetyo[1, 2], Bambang Soegijono[1, a)], Yusmaniar[3], and Musfirah Cahya Fajrah[4]

[1]*Departement of Physics, Universitas Indonesia, Depok 16424, Indonesia*
[2]*Departement of Mechanical Engineering, Universitas Negeri Jakarta, Jakarta 13220, Indonesia*
[3]*Departement of Chemistry, Universitas Negeri Jakarta, Jakarta 13220, Indonesia*
[4]*Departement of Physics, Institut Sains dan Teknologi Nasional, Jakarta 12640, Indonesia*

[a)]Corresponding author: naufal@ui.ac.id

Abstract. The coating of nickel (Ni) or Ni-alloy is one of the important metals for engineering applications. These materials have properties such as good corrosion resistance, ferromagnetic, good heat conduction. A few decades, numerous researches on electrodeposition of Ni from Watts's electrolyte solution have been reported. Therefore, in this research, Ni coated on polycrystalline copper (Cu) alloy substrates were prepared with various current density 3 mA/cm², 10 mA/cm², and 25 mA/cm² in watts solution to view more details about the effect of current density on the structure, morphology, and corrosion resistance of these films. The crystal structure, electrochemical behavior, and surface morphology were analyzed using X-Ray Diffraction (XRD), Potentiostat, and Scanning Electron Microscope (SEM) respectively. The difference in current densities affects crystallography parameters, electrochemical behaviors, and surface morphology of Ni layers. There are three major peaks exhibits as (111), (002), and (022) with cubic FCC crystal system and Fm-3m space group. The crystallite size of Ni film increases as the current density rise higher value. The highest corrosion rate is seen on the Ni-25 sample, and it is probably due to larger crystallite size and smaller polarization resistance. Increasing the current density has a significant influence on the reduction peak of Ni layers. As the current density increase, the peaks decrease. All the Ni layers display active-passive-transpassive behavior in 3.5% NaCl. All the Ni film produced shows electrochemically irreversible because the distance between oxidation and reduction peaks is more than 57 mV.

INTRODUCTION

There are currently many methods for surface modification, for example, electrodeposition, chemical vapor deposition, physical vapor deposition, and sputtering. Among them, electrodeposition is the cheapest, easy, eco-friendly method to produce single or multiple layers, which makes it very suitable for industrial production [1]. Commonly, electrodeposition of nickel (Ni) used watts electrolyte solution. A few decades, numerous researches on electrodeposition of Ni from watt's electrolyte solution have been reported. Electrodeposition Ni using watt's solution are resulting in good adhesion, various structure, and various grain sizes of the Ni layer [2–4]. The coating of Ni or Ni-alloy is one of the important metals for engineering applications. These materials have properties such as good corrosion resistance, ferromagnetic, good heat conduction [5–7]. Substrates and the electrodeposition parameters are mainly influenced by the evolution of the grain size and grain orientations [8]. Ni is commonly deposited on substrates such as Cu and brass [4,7]. The electrodeposition parameters that influenced the evolution of the grain orientations are usually electrolyte composition, current density, and stirring electrolyte during deposition.

There are several investigation reports for controlling the microstructure of the electrodeposited Ni layer. Yang-Tao et al. have electrodeposition of Ni by using industrial electrolytes with different time deposition. It was found, with the increases of deposition time, the adsorption atoms on the surface of the cathode and other diffusion atoms

The 2nd Science and Mathematics International Conference (SMIC 2020)
AIP Conf. Proc. 2331, 030017-1–030017-7; https://doi.org/10.1063/5.0041640
Published by AIP Publishing. 978-0-7354-4075-3/$30.00

are randomly encountered [9]. Wang et al. are resulting in different surface morphology, grain size, and peak intensity of electrodeposited Ni-graphene with various current density [10]. Moreover, increasing the current density would influence the crystallite size of the Ni layers [11]. As the current density increases, crystallite size would increases [12]. Electrodeposition of Ni at lower current density was resulting in the compact structure of morphology with less porosity [13]. The corrosion rate was affected by some behavior, i.e. passive layer. Park et al. found the increase of passive current density corresponding to increasing the corrosion rate [14]. Moreover, the micro strain is an important thing to be analyzed because the micro strain is certainty correspond to concentration defects in the sample, and this could be affected by the physical and chemical properties of the material [15].

The present work aims to electrodeposit Ni with different current densities. Polycrystalline Cu-alloy was used as a substrate with three variations of current densities as 3 mA/cm², 10 mA/cm², and 25 mA/cm². To obtained structure, electrochemical behavior, and surface morphology, the samples were analyzed with XRD, Potentiostat, and SEM.

METHOD

The polycrystalline Cu-alloy was used as substrates [4]. Cu-alloy substrates were cut into a size of 1cm x 1cm x 0.3cm. The substrates were sealed with epoxy resin, and a single side of the substrate was open. The substrate was ground successively by sandpapers with grit 500, 1500, and 3000, then cleaned in the ultrasonic cleaner, rinsed by distilled water, and finally dried. The electrodeposition process was carried out using the DC power supply. The anode was pure Ni sheet (99.9%) with an area twice of the cathode. Before to electrodeposition, the distance of the cathode and anode was maintained about 80 mm. The content of the electrolyte solution and parameter of the electrodeposition was presented in TABLE 1.

TABLE 1. Watts's solution content and temperature condition for electrodeposited Ni layer at different current densities.

Components	Contents (g/L)	Temperature (°C)	Electrolyte solution (mL)
$NiSO_4.6H_2O$	250		
$NiCl_2.6H_2O$	30	30	250
H_3BO_3	40		

XRD pattern was obtained by using a PANalytical Diffractometer (with CuKα radiation) and the 2θ with ranging from 20° to 90° at scan speed 0.02 step/second under condition voltage and current are 40 kV and 30 mA respectively. By using Highscore plus software, the XRD pattern obtained was analyzed to get the crystallographic parameter. The surface morphology of Ni layers was obtained using an SEM with magnification 5000 X.

The electrochemical behaviors of the Ni layers were carried out in terms of potentiostat equipment via Digi Ivy with standard three-electrode electrochemical cell in 3.5% NaCl solution with 30 °C temperature. The working electrodes area of 10 mm² were mounted in epoxy resin. The counter electrode was platinum, and the reference electrode was silver/silver chloride (Ag/AgCl). Electrochemical behaviors were separated into two investigations, potentiodynamic polarization to explore corrosion resistance of the Ni layer and cyclic voltammetry to obtained oxidation and reduction behavior of the Ni layers. The Ni layer was deposited on Cu alloy with current density 3, 10, and 25 mA/cm², and samples were named Ni-3, Ni-10, and Ni-25 respectively.

RESULT AND DISCUSSION

Structure

The XRD was carried out to investigate the influence of current density on crystallographic parameters of the electrodeposited Ni layers. For that purpose, the Ni layers were subjected to XRD corresponding to 2θ ranging from 20° to 90°. Two important aspects can be analyzed from diffraction patterns, such as relative peak intensity and crystallite size [16]. The XRD spectrums of electrodeposited Ni on various substrates are shown in Fig. 1. The peak of (111), (002), and (022) plane FCC crystal system with the different sizes were obtained base on XRD scans, which are consistent with the literature [1]. The Ni-10 and Ni-25 sample is shown a strong (002) plane. Others peak such as (111) and (022) plane are show weak intensities, whereas the (022) plane is very weak intensity. Moreover, the intensities of (022) planes are not influenced while the current densities change.

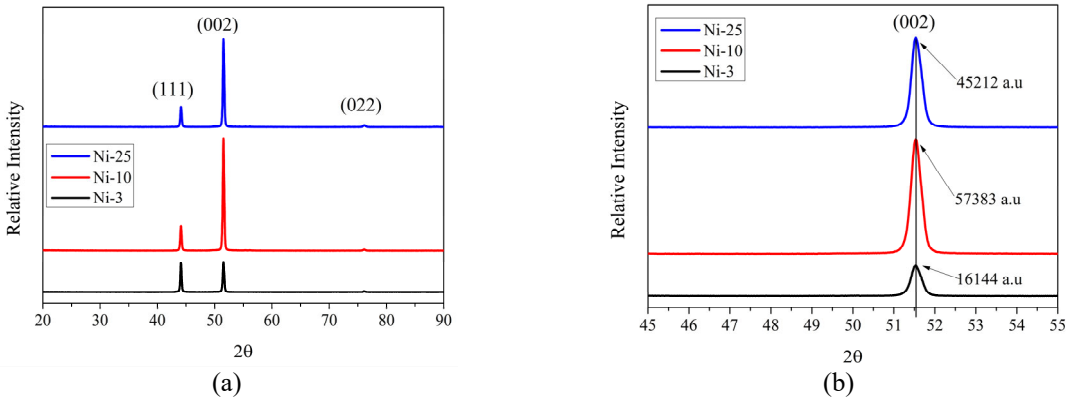

FIGURE 1. XRD spectrum (a) Electrodeposited Ni layer at different current densities (b) Difference intensity of (002) plane

As we can see in Fig. 1 (a), the increase in current density slightly influence on (111) plane but does not influence (022) plane. Whereas a significant influence (002) plane, by the increase in the current density changes the peak intensities (see FIGURE 1 (b)). This phenomenon is similar to other research that was coating Ni with various current density [11]. Based on JCPDS 96-901-3028, 2θ of Ni (111), (002), and (022) are at 44.16°, 51.45°, and 75.74° respectively. The (111), (002), and (022) plane of Ni layers is around 44.11, 51.5°, and 76.23°, there is no shifting 2θ position by increase the current density. The intensity of Ni-3, Ni-10, and Ni-25 are 16114 a.u, 57383a.u, and 45212a.u respectively (see Fig. 1 b). Nasirpouri et al. have found a reduction of the (002) plane would effectively decrease the crystallite size [17]. The crystallographic parameters on the Ni layer at different current densities are presented in TABLE 2.

TABLE 2. Crystallographic parameters of Ni layer at different current densities.

Element	Samples		
	Ni-3	**Ni-10**	**Ni-25**
Crystal System	Cubic FCC	Cubic FCC	Cubic FCC
Space Group	Fm-3m	Fm-3m	Fm-3m
a=b =c(Å)	3.4998	3.5005	3.5042
V (Å^3)	42.868	42.892	43.029
ρ (g cm^{-3})	9.09	9.09	9.06
Crystallites size (A°)	384.7	396.2	404.1
Micro strain (%)	0.000	0.000	0.000
R_{wp} (%)	6.66	8.61	8.63
GOF	1.21	2.54	2.25

Crystallographic parameters are based on refinement with high score software with Rwp and GOF below 9% and 2.6 respectively. To calculate the crystallite size of the Ni layer, the Scherrer equation was used like the following equation below (16):

$$\beta = 0.94\lambda/(d \times \cos\theta) \quad (1)$$

Where β is the peak broadening (rad), λ is the wavelength (A°), d is crystal size (A°), and θ is peak position. As we can see in table 2, it exhibits different volumes and density when electrodeposition of Ni layer at different current densities. The Ni-25 sample has less volume and density than the Ni-10 and Ni-3 samples. These indicated that the transferring rate of Ni species on the different current density are not similar. Electrodeposition with higher current density is associated with a higher nucleation rate [13]. This probably would be affected by the volume and density of the Ni layers.

The crystallite size of the Ni layer increases as the current density shift to a higher value, which results from the evolution of more hydrogen at the cathode interface [18]. A continuous increase of the crystallite size versus the current density for DC electrodeposition of Ni layers has also been recognized in other research [11]. The lowest crystallite size was found on the Ni-3 sample because the (002) plane is less than the others sample [17] and

attributed to decrease Ni ions concentration on the plating bath [12]. Less crystallite size offers benefits such as better corrosion resistance, wear, and hardness [19]. The micro strain is seen 0% for all samples, so this indicated no crystal defect on the Ni layers produced from different current densities [15].

Electrochemical Behavior

Potentiodynamic Polarization

Fig. 2 shows the potentiodynamic polarization curve of samples in 3.5% NaCl at 30°C solution temperature. Generally, there are phenomena active-passive-transpassive for all samples (Fig. 2 b). The phenomena active-passive-transpassive of the various samples are different. Nasirpory et al. also reported passive layers are the main factors that affected corrosion rate [17].

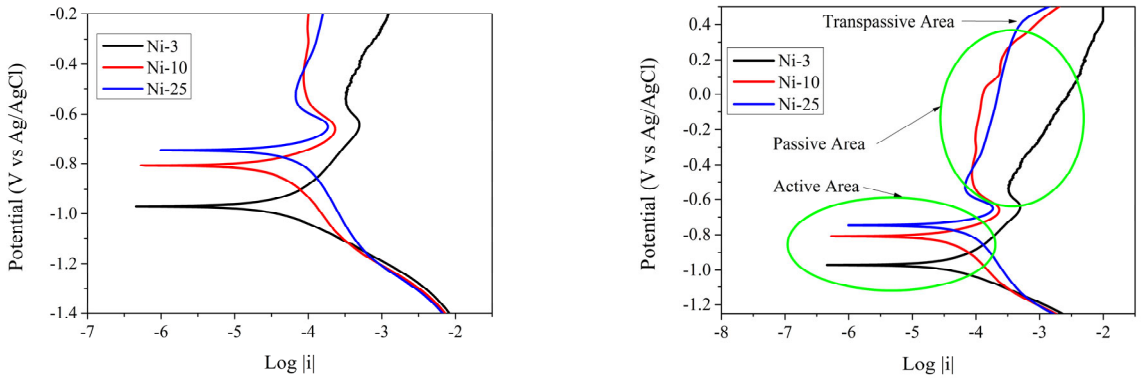

FIGURE 2. Potentiodynamic polarization curve Ni layer on various current densities at 3.5% NaCl (a) corrosion potential, and (b) Active-passive-transpassive area.

Fig. 2 (a) presents the corrosion potential of the samples. The corrosion potential is sifting to positive value as the current density increase. The Ni-25 sample has more positive corrosion potential than the other sample. This is indicated that higher current density leads to a higher deposition rate which results in a shift to more positive corrosion potential of a sample. Fig. 2 (b) presents active-passive-transpassive behavior of the samples. The Ni-3 sample seems to have a different passive area and more shift to the left side than two other samples.

The value of the corrosion rate was calculated using the following equation [20]:

$$Corr\ Rate = \mathrm{K1} \times \frac{i_{corr}}{D} \times EW \qquad (2)$$

Where, K1 (Constant) is 0.00327 mm g/μA cm yr, *Corr Rate* is the corrosion rate (mmpy), i_{corr} is the corrosion current density (μA/cm²), *EW* is the equivalent weight, and *D* is density (g/cm³). The value of the corrosion potential (E_{corr}), corrosion current density (i_{corr}), polarization resistance, and corrosion rate are summarized in TABLE 3.

TABLE 3. Corrosion current, corrosion potential, polarization resistance, and corrosion rate of Ni layer obtained from potentiodynamic polarization curves at different current densities.

Sample	i_{Corr} (μA/cm²)	E_{Corr}(V)	R_{ct} (Ohm)	Corr Rate (mmpy)
Ni-3	17.5	-0.874	1.471×10^{3}	0.203
Ni-10	28.3	-0.808	9.757×10^{2}	0.328
Ni-25	49.3	-0.746	4.397×10^{2}	0.572

Corrosion rate behaviors are different for each sample. The highest corrosion rate is seen in the Ni-25 sample, and Ni-3 has the lowest corrosion rate. The lowest corrosion rate is corresponding to phenomena of the passive areas, which has passive areas more shift to the right side that is not owned by the other samples. This is contradictory with Park et al. result, which results in a shift to more left side direction offer benefit better corrosion resistance [14]. Moreover, the Ni-3 sample has less crystallite size and higher polarization resistance than others. Those can be a benefit such as better corrosion resistance for the sample [19].

Fig. 3 shows the cyclic voltammetry graph of samples in 3.5% NaCl. Cyclic voltammetry clearly shows the presence of reduction and oxidation peaks corresponds to the deposition and re-dissolution [1].

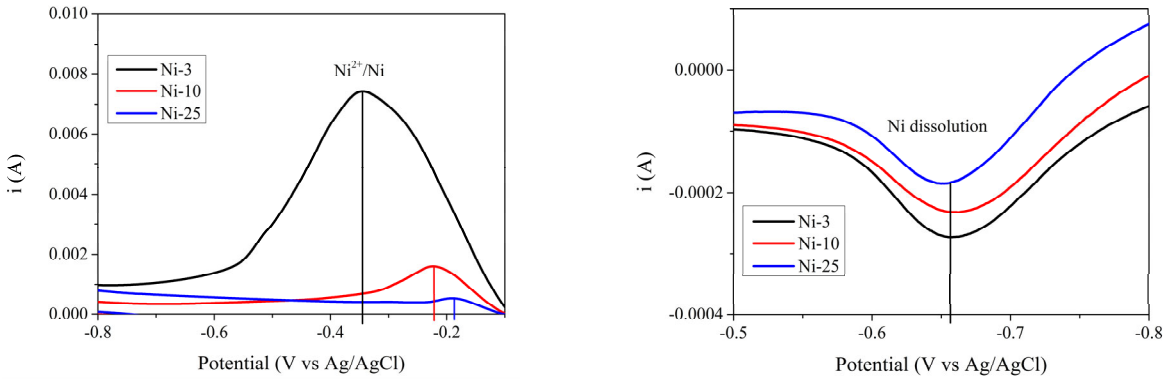

FIGURE 3. Cyclic voltammetry curves measurement at 3.5% NaCl for various current densities Ni layer (a) Reduction and (b) oxidation

For reduction reaction of Ni layer is presented in equation (3) and the oxidation of the Ni layer is presented in equation (4) below [4].

$$Ni^{2+} + 2e^{-} \rightarrow Ni \quad (3)$$

$$Ni \rightarrow Ni^{2+} + 2e^{-} \quad (4)$$

For the Ni-3 sample, the cyclic voltammetry shows that there are oxidation and reduction process which corresponding to oxidation from Ni to Ni2+ at the potential onset of −0.657 V followed by the reduction Ni2+ to Ni at the potential -0.369 V. Shifting the current density into 10 mA/cm² and 25 mA/cm² leads to the decrease of the reduction peak, corresponding to the reduction potential -0.224 V and -0.190 V respectively. This means need higher current to form Ni layer at sample Ni-3 from Ni^{2+}. Moreover, the higher the current density, the more it will shift towards a more positive potential of reduction. The Ni-3 negative potential reduction is higher than Ni-10 and Ni-25 samples. This is probably due to a higher nucleation rate is form leads to higher negative reduction potential [11]. Moreover, shifting the current density also affected the oxidation potential sample Ni-10 and Ni-25 to -0.663 V and -0.652V.

There are different distances between the oxidation and reduction peak of each sample (see Fig. 3 a and b). A shift to higher current density leads to an increase in distance between oxidation and reduction peak. The distance between oxidation and reduction peaks for Ni-3, Ni-10, and Ni-25 is 0.288V, 0.439V, and 0.462V respectively. Those are indicating the sample is irreversible electrochemical reaction because of the distance between oxidation and reduction peaks more than 57 mV [21].

Surface Morphology

The influences of current densities on Cu alloy substrates are presented in Fig. 4. A typical pyramidal colony structure is shown, which size changes within an increase in the current densities. The smaller and homogeneity of pyramidal colonies with crevice on the surface which shown in the Ni-3 sample was similar to other research [11]. Based on Fig. 3(a), there is a higher negative potential reduction of Ni-3 sample. The higher potential of reduction results in a higher nucleation rate and thus would affect a grain refinement [11]. Moreover, lower current density commonly shows more compact structures of morphology with lower porosity value [13]. Change the current density to 10 mA/cm² influence the pyramidal colony grows rapidly resulting in the highest grain size. The Ni-10 sample shows huge and homogeneity of pyramidal colonies form. Moreover, the pyramidal colony structure slightly decreases affected by shifting the current density to 25 mA/cm². The big pyramidal colonies are surrounded by small pyramidal colonies, and the sides of the pyramidal colonies are smooth without crevice is shown in the Ni 25 sample. Compared using XRD evaluation, there is the smallest intensity of (002) plane on Ni-3 followed by Ni-25

and Ni-10. There is a correlation between intensities of (002) plane and grain size. The strong intensity of the (002) plane is closely related to grain size [18]. The Ni-3 has less grain size than Ni-10 because of the lowest (002) plane intensity than the other samples. The Ni-10 has a bigger grain size than other samples because it has highest the (002) plane intensity than the other samples.

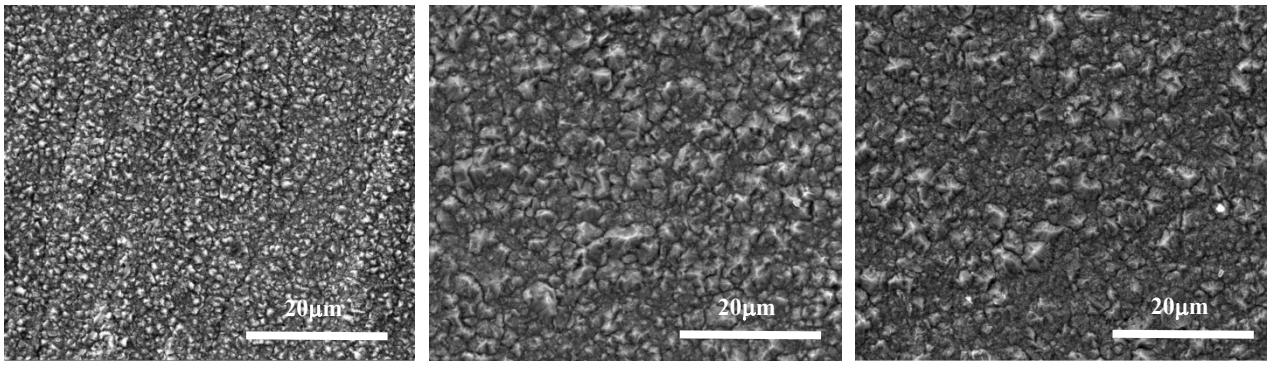

(a) (b) (c)

FIGURE 4. SEM image showing comparison electrodeposited Ni layer on various current densities (a) Ni-3, (b) Ni-10, and (c) Ni-25

CONCLUSION

Ni coated on various substrates with various current densities was successfully done. The differences of current densities are significant affecting crystallography parameters, electrochemical behaviors, and surface morphology of Ni layers. There are three major peaks exhibits as (111), (002), and (022) with cubic FCC crystal system and Fm-3m space group. The crystallite size of Ni film increases as the current density shift to a higher value. All the Ni layers display active-passive-transpassive behavior in 3.5% NaCl when potentiodynamic polarization was performed. The highest corrosion rate is seen on the Ni-25, which is probably due to larger crystallite size and smaller polarization resistance than others. Increasing the current density has a significant influence on the reduction peak of Ni layers. As the current density increase, the peaks decrease. The various samples showed irreversible electrochemical reactions because of the distance between oxidation and reduction peaks of more than 57 mV.

ACKNOWLEDGMENT

This research was supported by Ministry of Research, Technology and Higher Education of the Republic of Indonesia Doctoral dissertation research grants No: NKB-1825/UN2.R3.1/HKP.05.00/2019.

REFERENCES

1. C. D. Gu, Y. H. You, Y. L. Yu, S. X. Qu, and J. P. Tu, *Surf Coatings Technol.* **205** (21–22), pp. 4928–4933 (2011).
2. Z. Shafiee, M. E. Bahrololoom, and B. Hashemi, *Mater Des.* **108**, pp. 19–26 (2016).
3. A. M. Rashidi, *J Mater Sci Technol* **28** (12), pp. 1071–1076 (2012). doi: http://dx.doi.org/10.1016/S1005-0302(12)60175-3
4. F. B. Susetyo, A. Faridh, and B. Soegijono, *IOP Conference Series: Materials Science and Engineering* **694** (1), p. 012040 (2019).
5. Z. Yang, X. Liu, and Y. Tian, *Colloids Surfaces A Physicochem Eng Asp* **560**, pp. 205–212 (2019). doi: https://doi.org/10.1016/j.colsurfa.2018.10.024
6. A. Lelevic and F. C. Walsh, *Surface and Coatings Technology* **378**, p. 124803 (2019); doi: https://linkinghub.elsevier.com/retrieve/pii/S0257897219307479
7. F. B. Susetyo, M. C. Fajrah, and B. Soegijono, *e-Journal Surf Sci Nanotechnol.* **18**, pp. 223–230 (2020).
8. H. Alimadadi, A. B. Fanta, T. Kasama, M. A. J. Somers, and K. Pantleon, *Surf Coatings Technol* **299**, pp. 1–6 (2016). doi: http://dx.doi.org/10.1016/j.surfcoat.2016.04.068

9. X. Yang-tao, D. Yu-jie, Z. Wei, and Z. Tian-dong, *Surf Coatings Technol* **330**, pp. 170–177 (2017). doi: http://dx.doi.org/10.1016/j.surfcoat.2017.09.078
10. J. Wang, *et al.*, *Surf Coatings Technol* **358**, pp. 765–774 (2019).
11. Y. R. Uhm, K. Y. Park, and S. J. Choi, *Res Chem Intermed.* **41** (7), pp. 4141–4149 (2015).
12. A. M. Rashidi and A. Amadeh, *J Mater Sci Technol* **26** (1), pp. 82–86 (2010). doi: http://dx.doi.org/10.1016/S1005-0302(10)60013-8
13. V. F. C. Lins, E. S. Cecconello, and T. Matencio, *J Mater Eng Perform.* **17** (5), pp. 741–745 (2008).
14. K. Park, S. Ahn, and H. Kwon, *Electrochim Acta* **56** (3), pp. 1662–1669 (2011). doi: http://dx.doi.org/10.1016/j.electacta.2010.09.077
15. K. Maniammal, G. Madhu, and V. Biju, *Phys E Low-Dimensional Syst Nanostructures* **85**, pp. 214–222 (2017). doi: http://dx.doi.org/10.1016/j.physe.2016.08.035
16. N. P. Wasekar, P. Haridoss, S. K. Seshadri, and G. Sundararajan, *Surf Coatings Technol.* **291**, (2016).
17. F. Nasirpouri, *et al.*, *Appl Surf Sci* **292**, pp. 795–805 (2014).
18. H. Zhao, L. Liu, J. Zhu, Y. Tang, and W. Hu, *Mater Lett.* **61** (7), pp. 1605–1608 (2007).
19. C. R. Thurber, *et al.*, *Curr Appl Phys* **16** (3), pp. 387–396 (2016).
20. N. Elangovan, S. Pugalmani, A. Srinivasan, N. Rajendiran, and N. Rajendran, *e-Journal Surf Sci Nanotechnol.* **16**, pp. 5–13 (2018).
21. N. Elgrishi, K. J. Rountree, B. D. McCarthy, E. S. Rountree, T. T. Eisenhart, and J. L. Dempsey, *J Chem Educ.* **95** (2), pp. 197–206 (2018).